ELSEVIER

Earth and Planetary Science Letters 196 (2002) 161–174

EPSL

www.elsevier.com/locate/epsl

# Thorium isotopes in the western Mediterranean Sea: an insight into the marine particle dynamics

M. Roy-Barman *, L. Coppola, M. Souhaut

*LEGOS, 14, Avenue Edouard Belin, 31400 Toulouse, France*

Received 19 July 2001; received in revised form 21 November 2001; accepted 5 December 2001

**Abstract**

We present a detailed view of the $^{230}$Th–$^{232}$Th systematics in the western Mediterranean Sea in order to constrain water and particle fluxes. The conclusions obtained at the regional scale are also relevant at a more global scale although they may be more difficult to establish in the open ocean. $^{230}$Th and $^{232}$Th were analyzed in size-fractionated seawater and marine particle samples collected in the Ligurian, Alboran and Ionian seas. The $^{230}Th_{xs}$ ($^{230}$Th produced by the radioactive decay of $^{234}$U in seawater) profiles at DYFAMED and in the Alboran sea site are not linear due to the formation of deep waters. The difference of $^{230}Th_{xs}$ concentration between these two sites is related to the aging of the water masses and to different scavenging conditions. The $^{230}$Th/$^{232}$Th ratio is used as a tracer during mixing processes to provide information on the pathways followed by the matter in the water column. At DYFAMED, filtered ($< 0.2$ μm) and ultrafiltered ($< 1$ kDa) solutions have similar $^{230}$Th/$^{232}$Th ratios, suggesting that an equilibrium exists between truly dissolved and colloidal Th. The change of the Th flux and of the $^{230}$Th/$^{232}$Th ratio of trapped particles observed in August between 200 m and 1000 m is best explained by aggregation of filtered large particles on the trapped particles. The residence time of filtered large particles with respect to aggregation on trapped particles is of the order of 8–80 days. The combined budget of $^{230}$Th and $^{232}$Th inputs to the western Mediterranean Sea requires the dissolution of 3–5% of the Th associated with all the continental particulate inputs (including particles sequestered in margins) suggesting that eolian inputs are not the only source of refractory elements to the Mediterranean Sea and may be to the whole ocean. 

*Keywords:* thorium; isotopes; sea water; particles; sedimentation; Mediterranean Sea

## 1. Introduction

Understanding the particle dynamics in the western Mediterranean Sea has strong implications for the local carbon cycle [1] and the fate of anthropogenic pollutants [2]. Particulate transport involves physical, chemical and biological processes and sometimes non-steady-state conditions [1–4]. Thorium isotopes can be used to constrain these processes because: (1) Th is insoluble and strongly associated with the particulate matter and (2) the inputs of Th short-lived isotopes by radioactive decay are precisely known. The study of $^{234}$Th ($t_{1/2} = 24$ days) in the Ligurian Sea indicates that particle removal from the sur-

* Corresponding author. Present address: LSCE, Domaine du CNRS, 91198 Gif sur Yvette Cedex, France. Tel.: +33-1-6182-3566; Fax: +33-1-6182-3568.
*E-mail address:* matthieu.roy-barman@lsce.cnrs-gif.fr (M. Roy-Barman).

0012-821X/02/$ – see front matter 
PII: S0012-821X(01)00606-9

face water is controlled by zooplankton grazing [5]. Other thorium isotopes with longer half-lives such as $^{232}$Th ($t_{1/2} = 1.4 \times 10^{10}$ yr) and $^{230}$Th ($t_{1/2} = 75\,000$ yr) can bring additional and distinct information, because $^{232}$Th (derived from continental material) and $^{230}$Th (mostly produced in situ by radioactive decay of $^{234}$U in seawater) have distinct sources in the ocean [6]. $^{230}$Th and $^{232}$Th data in the Mediterranean Sea are very scarce [7,8]. We report the first extensive data set of $^{230}$Th and $^{232}$Th in size-fractionated samples from the western Mediterranean Sea. First, we use the $^{230}$Th chronometer [9] to evaluate $^{230}$Th scavenging rates and the influence of water mixing on the $^{230}$Th profiles. Then, we use the $^{230}$Th/$^{232}$Th ratio as a source tracer during processes involving mixing of matter from different origins (solution/colloid interactions, aggregation of particles). The $^{230}$Th chronometer and the $^{230}$Th/$^{232}$Th ratio are combined to evaluate the flux of $^{232}$Th in seawater by dissolution of lithogenic material.

## 2. Sampling and analytical procedure

### 2.1. Sampling

The DYFAMED (DYnamique des Flux Atmosphériques en MEDiterranée) station (Fig. 1) is located in the western basin of the Mediterranean Sea, 30 nautical miles (54 km) off Nice (43°25′N, 07°54′E, maximum depth: 2200 m). This site was chosen to study the vertical transport of particulate matter in the water column from the surface to the sediment because it receives strong eolian inputs but it is protected from direct riverine inputs by the Ligurian current. Unfiltered, filtered (0.2 μm) and ultrafiltered (1000 Da) seawater samples and filtered large (> 60 μm) particles were collected on a vertical profile at the end of the summer of 1996 at the DYFAMED site. Seawater was collected with 30 l Niskin bottles. Depths were determined with SIS pressure sensors. Some seawater samples were filtered on board with a Sartorius cross-flow filtration system associated with a 0.2 μm filtration cartridge. Filtered and unfiltered samples were acidified on board to prevent Th sorption on the container walls. Some filtered samples remained unacidified and were ultrafiltered one month later with the Sartorius cross-flow filtration system associated with a 1 kDa polysulfone filtration cartridge [10]. Initially, the membrane was cleaned with NaOH 2%, distilled water, $H_3PO_4$ 0.1% and distilled water. Between samples, 500 ml of distilled water and a 1 l aliquot of the sample to be analyzed were passed to precondition the membrane but the filtrate was discarded. Then, the sample was processed and the filtrate was recovered for analysis. Colloids were concentrated in the retentate by a factor 5–10 but they were not analyzed. Large particles were collected by filtration on Teflon grids (diameter: 142 mm, pore size 60 μm) with in situ pumps (MARK II, Challenger

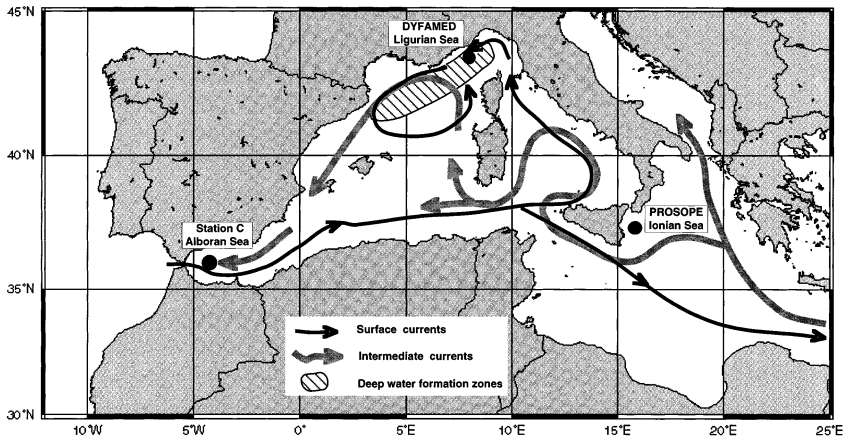


Fig. 1. Location of the sampling sites.

Oceanic). Particulate matter was collected at 200 and 1000 m during the 1994 DYFAMED sediment trap time series. The treatment of the trapped material is published elsewhere [1]. Trapped particles from three periods were analyzed: from 25 January to 9 February and from 24 February to 11 March (bloom period); from 24 August to 8 September (oligotrophic conditions).

Seawater and small filtered particle samples were collected during the Alboran Sea HFF experiment (WP2-T213) at Station C (36°0′16″N, 4°15′58″W, maximum depth: 1270 m). Unfiltered seawater samples were acidified on board. Small particles were collected by filtration of large volumes of seawater on Durapore filters (diameter: 142 mm, pore size 0.6 μm) with in situ pumps (MARK II, Challenger Oceanic).

An unfiltered seawater sample was collected in the Ionian basin, South of Mecine Strait (Prosope cruise, Station 15, 37°22.523′N and 15°36.729′E, maximum depth: 2148 m) to characterize the water flowing from the eastern basin to the western basin.

### 2.2. Chemical analyses

#### 2.2.1. Seawater

$^{229}$Th and Fe carrier were added to the seawater samples. After a week of isotopic equilibration, pH was raised to 8–9 with $NH_3$ to produce $Fe(OH)_3$. The precipitate was recovered by centrifugation and dissolved in $HNO_3$. The resulting solution was centrifuged to remove a residual $SiO_2$ gel. This gel was dissolved in a $HF+HNO_3+HClO_4$ mixture, dried and re-dissolved in $HNO_3$. The supernatant and the solution resulting from the precipitate dissolution were mixed together and passed through anionic ion exchange columns to purify Th [6]. For 10 l of seawater, blanks are $^{232}Th = 58 \pm 20$ pg (blank correction = 5%) and $^{230}Th = 0.25 \pm 0.17$ fg (blank correction = 1%) for unfiltered samples, $^{232}Th = 179 \pm 20$ pg (blank correction = 6–12%), $^{230}Th = 1.1 \pm 0.5$ fg (blank correction = 1–7%) for filtered samples and $^{232}Th = 263 \pm 65$ pg (blank correction = 13–28%) and $^{230}Th = 4 \pm 1$ fg (blank correction = 4–17%) for ultrafiltered samples.

#### 2.2.2. Particles

Large filtered particle samples were placed in a hot 5% HCl solution for a day to remove the particles from the Teflon grids. The particles were dissolved in aqua regia. For bulk samples, this solution was dried and the residue was dissolved in $HNO_3$ 16 N. Residual solids were separated by centrifugation, dissolved in $HF$-$HNO_3$-$HClO_4$, dried and re-dissolved with $HNO_3$ 16 N. The separation prevented the $Ca^{2+}$ ions released in HCl and aqua regia from precipitating as $CaF_2$. After complete dissolution of the residual solids, the two solutions were mixed back together. For some samples, the aqua regia leachate and the residual particles were analyzed separately in an attempt to separate the authigenic and lithogenic fractions. Trapped particles collected at DYFAMED were dissolved in 1 ml of aqua regia. The solution was dried and the residue was dissolved in $HF$-$HNO_3$-$HClO_4$, dried and dissolved in $HNO_3$ 16 N. The filtered suspensions from the Alboran Sea were leached with 25% acetic acid to separate the authigenic Th from the lithogenic fraction. For all the particulate samples, after complete dissolution, $^{229}$Th spike was added and the Th was purified with an anionic ion exchange column [6]. Typical blanks are $^{232}Th = 40 \pm 20$ pg (blank correction = 0–12%) and $^{230}Th = 0.6 \pm 0.4$ fg (blank correction = 0–33%), except for acetic acid leachates where blanks are $^{232}Th = 55 \pm 15$ pg (blank correction = 8–81%) and $^{230}Th = 1.3 \pm 1.3$ fg (blank correction = 100%).

### 2.3. Mass spectrometry

Purified Th was analyzed by TIMS on a Finnigan Mat 261 mass spectrometer equipped with a Spectromat ion counting system. Samples were loaded on single filaments with a colloidal graphite matrix [6]. All isotopes were measured by peak-switching on an ion counter. The abundance sensitivity at 2 mass unit was typically 0.7 ppm. This contribution was corrected by measuring the baseline on mass 229.5 and mass 230.5 and by subtracting the mean value from the signal measured on mass 230. For a sample with $^{230}Th/^{232}Th$ as low as $4.5 \times 10^{-6}$ (the least favorable case), there was a 16% correction and we estimate that

Table 1
Th isotope concentrations in seawater at the DYFAMED site

| Depth (m) | Volume (l) | $^{232}$Th (pg/kg) | $^{230}$Th (fg/kg) | $^{230}$Th/$^{232}$Th ($\times 10^6$) | $^{230}$Th$_{xs}$ (fg/kg) |
|---|---|---|---|---|---|
| Unfiltered samples | | | | | |
| 20 A | 11 | 285 ± 4 | 3.7 ± 0.1 | 13.0 ± 0.5 | 2.4 ± 0.2 |
| 200 A | 11 | 249 ± 7 | | | |
| 200 B | 11 | 247 ± 3 | 3.6 ± 0.1 | 14.7 ± 0.5 | 2.5 ± 0.1 |
| 500 A | 10 | 377 ± 17 | 7.6 ± 1.3 | 20 ± 5 | 5.9 ± 1.4 |
| 1000 A1 | 5 | 221 ± 6 | 6.2 ± 0.2 | 28.1 ± 1.4 | 5.2 ± 0.3 |
| 1000 A2 | 6 | 209 ± 7 | 5.7 ± 0.2 | 27.3 ± 1.4 | 4.7 ± 0.3 |
| 1000 B | 11 | 235 ± 5 | 5.9 ± 0.2 | 25.4 ± 1.2 | 4.9 ± 0.3 |
| 1500 A | 11 | 171 ± 4 | 4.5 ± 0.1 | 26.7 ± 1.0 | 3.8 ± 0.1 |
| 2000 A | 12 | 152 ± 4 | 6.0 ± 0.2 | 40.1 ± 1.4 | 5.4 ± 0.2 |
| Filtered samples (< 0.2 μm) | | | | | |
| 20 A | 10 | 181 ± 4 | 2.5 ± 0.2 | 13.9 ± 1.1 | 1.7 ± 0.2 |
| 20 A | 11 | 198 ± 3 | 2.2 ± 0.3 | 11.3 ± 1.4 | 1.3 ± 0.3 |
| 75 A | 11 | 219 ± 4 | 2.0 ± 1.8 | 9.3 ± 8 | 1 ± 2 |
| 200 A | 11 | 229 ± 4 | 3.4 ± 0.2 | 15.1 ± 0.7 | 2.4 ± 0.2 |
| 500 A | 10 | 212 ± 4 | 4.4 ± 0.3 | 20.7 ± 1.5 | 3.4 ± 0.3 |
| 1000 A1 | 6 | 176 ± 4 | 5.0 ± 0.2 | 28.6 ± 1.5 | 4.2 ± 0.1 |
| 1000 A2 | 1 | 180 ± 23 | 5.1 ± 0.6 | 28.3 ± 5.0 | 4.3 ± 0.7 |
| 1000 A3 | 1 | 176 ± 21 | 4.5 ± 0.6 | 25.7 ± 4.5 | 3.7 ± 0.7 |
| 1500 A | 10 | 174 ± 10 | 4.8 ± 0.3 | 27.8 ± 2.3 | 4.0 ± 0.3 |
| 2000 A | 10 | 145 ± 10 | 3.9 ± 0.2 | 29.2 ± 2.5 | 3.6 ± 0.3 |
| Ultrafiltered samples (< 1 kDa) | | | | | |
| 20 | 9 | 106 ± 10 | 1.5 ± 0.4 | 14 ± 4 | 1.0 ± 0.4 |
| 200 | 7 | 84 ± 11 | 2.0 ± 0.5 | 24 ± 8 | 1.7 ± 0.5 |
| 1000 | 6 | 138 ± 10 | 2.6 ± 0.2 | 19 ± 3 | 2.0 ± 0.2 |

the non-linearity of the baseline introduced less than 4% of error (which is less than the statistical uncertainty for the samples with low $^{230}$Th/$^{232}$Th ratios). For samples with higher ratios, this baseline contribution becomes very low. The agreement between the measured $^{230}$Th/$^{232}$Th ratio and the recommended value [11] of a Th standard indicates that the accuracy of the TIMS measurement is typically better than 2%.

Table 2
Th isotopes in large filtered particles (> 60 μm) collected at the DYFAMED site

| Sample | Depth (m) | Filtered volume | $^{232}$Th (pg/kg) | $^{230}$Th (fg/kg) | $^{230}$Th/$^{232}$Th ($\times 10^6$) | $^{230}$Th (fg/kg) |
|---|---|---|---|---|---|---|
| DYF5 bulk | 25 | 1566 | 2.36 ± 0.02 | 0.0145 ± 0.0012 | 6.2 ± 0.5 | 0.0042 |
| DYF10 leachate | 25 | 1195 | 2.12 ± 0.11 | 0.0110 ± 0.0022 | 5.2 ± 1.3 | 0.0015 |
| DYF10 residue | 25 | 1195 | 0.37 ± 0.004 | 0.0017 ± 0.0007 | 4.6 ± 1.9 | 0.00004 |
| DYF3 bulk | 990 | 761 | 8.53 ± 0.07 | 0.087 ± 0.004 | 10.3 ± 0.5 | 0.0490 |
| DYF1 bulk | 1000 | 667 | 9.71 ± 0.09 | 0.113 ± 0.009 | 11.7 ± 1.0 | 0.0696 |
| DYF9 leachate | 990 | 767 | 6.03 ± 0.05 | 0.0710 ± 0.0015 | 11.9 ± 0.3 | 0.0441 |
| DYF9 residue | 990 | 767 | 0.90 ± 0.00 | 0.0054 ± 0.0004 | 6.1 ± 0.5 | 0.0014 |
| DYF7 leachate | 1010 | 835 | 7.27 ± 0.03 | 0.080 ± 0.002 | 11.1 ± 0.4 | 0.0473 |
| DYF7 residue | 1010 | 835 | 0.95 ± 0.02 | 0.0063 ± 0.0008 | 6.7 ± 1.0 | 0.0021 |

Th present in soluble phases was separated from Th present in more refractory mineral by dissolution of the soluble phases in aqua regia. These dissolutions yielded a leachate and a residue. Th present in soluble phases was analyzed in the leachate whereas Th present in refractory phases was analyzed in the residue. For bulk analysis, the leachate and residue were mixed together prior to analysis (see text for details).

Table 3
Th isotope concentrations in the DYFAMED sediment trap time series

| Date (1994) | Depth (m) | Mass flux (mg/m$^2$/day) | $^{232}$Th (μg/g) | $^{230}$Th (pg/g) | $^{230}$Th/$^{232}$Th ($\times 10^6$) | $^{230}$Th$_{xs}$ [a] (pg/g) | $^{230}$Th$_{xs}$ flux (pg/m$^2$/yr) |
|---|---|---|---|---|---|---|---|
| 25/01–09/02 | 200 | 101 | 15.1 ± 0.2 | 77 ± 6 | 5.1 ± 0.4 | 11 | 412 |
| 25/01–09/02 | 1000 | 106 | 10.4 ± 0.1 | | | | |
| 24/02–11/03 | 200 | 149 | 8.6 ± 0.08 | 39 ± 3 | 4.6 ± 0.3 | 1.3 | 73 |
| 24/02–11/03 | 1000 | 363 | 10.8 ± 0.1 | 55 ± 3 | 5.1 ± 0.3 | 7.3 | 973 |
| 24/08–08/09 | 200 | 15 | 1.78 ± 0.02 | 10.6 ± 0.6 | 6.0 ± 0.3 | 2.9 | 15 |
| 24/08–08/09 | 1000 | 19 | 4.66 ± 0.02 | 35 ± 2 | 7.7 ± 0.3 | 15 | 103 |

[a] Based on $^{230}$Th/$^{232}$Th = $4.4 \times 10^{-6}$ in the lithogenic material.

## 3. Results

$^{230}$Th and $^{232}$Th concentrations in seawater and particle samples are given in Tables 1–4. Thorium concentrations are expressed in pg/kg for $^{232}$Th (1 pg/kg = 0.000246 dpm/$10^3$ kg) and in fg/kg for $^{230}$Th (1 fg/kg = 0.0459 dpm/$10^3$ kg) whereas all isotopic ratios are expressed in atoms/atoms. $^{230}$Th and $^{232}$Th profiles in seawater are shown in Fig. 2. At DYFAMED, $^{232}$Th concentrations range from 145 pg/kg to 229 pg/kg in filtered seawater and from 152 pg/kg to 377 pg/kg in unfiltered seawater. $^{230}$Th concentrations range from 2 fg/kg to 5.1 fg/kg in filtered seawater and from 3.6 fg/kg to 7.6 fg/kg in unfiltered seawater. Higher Th concentrations are found in the Alboran and Ionian seas: $^{232}$Th concentrations in unfiltered seawater range from 321 pg/kg to 517 pg/kg and $^{230}$Th concentrations range from 6.3 fg/kg to 18.1 fg/kg. Replicates made on some filtered and unfiltered samples of different sizes demonstrate the good reproducibility of the results. The $^{232}$Th content of the Mediterranean samples is on the high side of the Atlantic values (22–349 pg/kg [12]) reflecting the strong local contribution of continental inputs. The $^{230}$Th content of the Mediterranean samples is equal or higher than the Atlantic values (2–9 fg/kg between 0 and 2000 m [12]) and significantly higher than in the Mauritania upwelling (0.5–2.4 fg/kg between 0 and 2000 m [13]). The $^{230}$Th/$^{232}$Th ratios of seawater range from $9 \times 10^{-6}$ to $40 \times 10^{-6}$ at DY-

Table 4
Th isotope concentrations in the Alboran Sea and Ionian Sea

| Depth (m) | Volume (l) | $^{232}$Th (pg/kg) | $^{230}$Th (fg/kg) | $^{230}$Th/$^{232}$Th ($\times 10^6$) | $^{230}$Th$_{xs}$ (fg/kg) |
|---|---|---|---|---|---|
| *Alboran Sea* | | | | | |
| Unfiltered seawater | | | | | |
| 45 | 5 | 321 ± 26 | 6.5 ± 0.9 | 22.7 ± 1.5 | 5.0 ± 1 |
| 200 | 5 | 469 ± 26 | 12.6 ± 1 | 27 ± 2.6 | 10.5 ± 1 |
| 1000 | 5 | 517 ± 16 | 18.1 ± 2.2 | 35.3 ± 4.4 | 15.8 ± 2.3 |
| Filtered particles (> 0.6 μm): labile fraction | | | | | |
| 45 | 30 | 0.6 ± 0.8 | bdl | | |
| 200 | 80 | 4.5 ± 0.4 | bdl | | |
| 1000 | 200 | 2.0 ± 0.2 | bdl | | |
| Filtered particles (> 0.6 μm): refractory fraction | | | | | |
| 45 | 30 | 81 ± 3 | 0.80 ± 0.15 | 9.9 ± 2 | 0.44 ± 0.15 |
| 200 | 80 | 134 ± 2 | 0.68 ± 0.15 | 5.1 ± 1 | 0.09 ± 0.15 |
| 1000 | 200 | 140 ± 3 | 0.95 ± 0.08 | 6.8 ± 1 | 0.33 ± 0.09 |
| *Ionian Sea* | | | | | |
| Unfiltered sample | | | | | |
| 600 | 1.5 | 439 ± 16 | 6.3 ± 0.5 | 14.5 ± 1.6 | 4.4 ± 0.5 |

bdl: below detection limit.

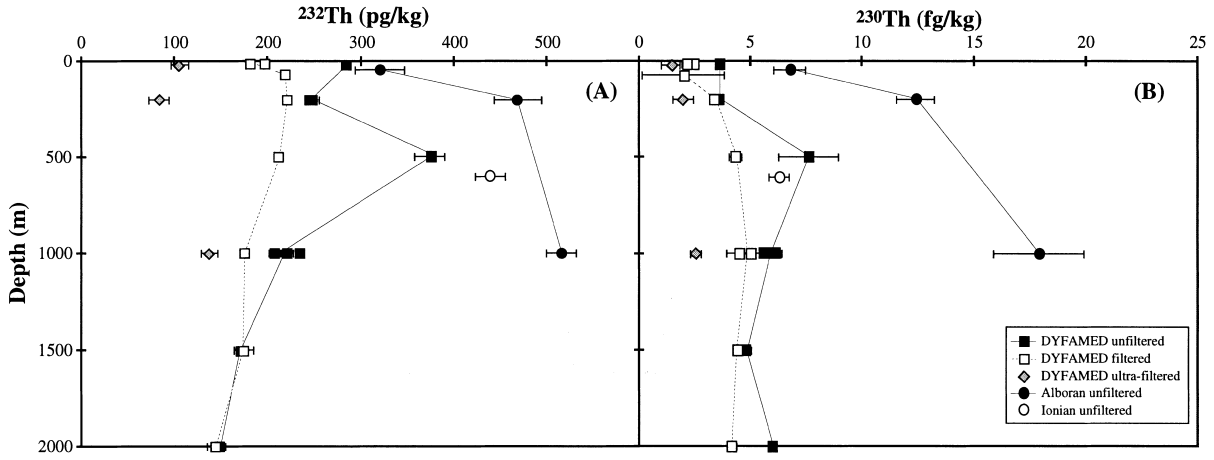


Fig. 2. Thorium isotope concentration profiles in water samples. (A) $^{232}$Th profile in pg/kg. (B) $^{230}$Th profile in fg/kg.

FAMED, from $23\times10^{-6}$ to $35\times10^{-6}$ in the Alboran Sea and a value of $14.5\times10^{-6}$ was measured in the Ionian Sea.

In the ocean, most $^{230}$Th is derived from the radioactive decay of $^{234}$U in seawater. However, when lithogenic inputs are high, the lithogenic $^{230}$Th contribution cannot be neglected. The $^{230}$Th produced by the in situ decay of $^{234}$U in seawater ($^{230}Th_{xs}$) is calculated by subtracting the lithogenic $^{230}$Th component to the total $^{230}$Th:

$$^{230}Th_{xs} = {}^{230}Th_{measured} - {}^{232}Th_{measured}\left(\frac{^{230}Th}{^{232}Th}\right)_{litho} \quad (1)$$

with $(^{230}Th/^{232}Th)_{litho} = 4.4\times10^{-6}$ based on a mean $^{232}Th/^{238}U = 3.8$ (atom/atom) of the continental crust [14] and on the $^{230}Th/^{232}Th$ ratio of lithogenic-rich particulate matter collected in the Ligurian Sea [15]. Hence, around 35% of the total $^{230}$Th has a lithogenic origin and only 65% is produced in situ in the 20 m seawater samples of DYFAMED (Table 1). The $^{230}Th_{xs}$ content in seawater is larger in the Alboran Sea than at DYFAMED indicating differences in the transport of Th between the two sites.

In the DYFAMED ultrafiltered samples, 36–78% of the $^{232}$Th and 47–77% of the $^{230}Th_{xs}$ present in the filtered samples are still present in the $<1$ kDa fraction. We cannot rule out that some truly dissolved Th was lost by adsorption on colloids or on the container walls during the month of storage or on the ultrafiltration membrane [16]. However, our results are consistent with the fraction of $^{234}$Th passing through 1 kDa membranes (25–89%) for experiments that do not involve long storage before ultrafiltration [17]. Even if adsorption occurred, it did not modify the $^{230}Th/^{232}Th$ ratio of the truly dissolved Th since both isotopes should be adsorbed at the same rate (isotopes of a heavy element have the same chemical behavior in solution) and it is legitimate to compare the $^{230}Th/^{232}Th$ ratios of the filtered and ultrafiltered solutions. Therefore, a key result is that the $^{230}Th/^{232}Th$ ratios of these solutions are not very significantly different.

Direct analysis of small filtered particles from the Alboran Sea indicates that 25–33% of the $^{232}$Th in the water column is associated with small filtered particles. Most particulate Th is not soluble in acetic acid indicating a refractory nature. The $^{230}Th/^{232}Th$ ratio is lower in these particles than in the surrounding water. At DYFAMED, the $^{232}$Th content (0–165 pg/kg or 0–43% of $^{232}$Th in seawater) and the $^{230}Th/^{232}Th$ ratio ($15\pm5$) of small particles can be estimated by comparing filtered and unfiltered samples. Large uncertainties on the $^{230}Th/^{232}Th$ ratios are due to small differences between the filtered and unfiltered water concentrations. At DYFAMED, filtered large particles contain less than 5% of the Th in seawater. The $^{230}Th/^{232}Th$ ratio of filtered large par-

ticles is significantly lower than the $^{230}Th/^{232}Th$ ratio of seawater. Aqua regia was used in an attempt to separate authigenic Th from silicate-bounded Th more efficiently than with acetic acid leaching. As expected, the refractory Th has a low $^{230}Th/^{232}Th$ ratio but the leachate may contain some lithogenic Th.

The $^{232}Th$ content of trapped particles (μg Th/g trapped particles) ranges from 1.8 to 15 μg/g (Table 4). For a given period, the $^{230}Th_{xs}$ flux increases with depth as expected for this in situ-produced particle-reactive long-lived isotope. More surprisingly, the $^{232}Th$ flux increases with depth in spring and summer, whereas a constant flux would have been expected for a lithogenic tracer. The significant increase of the $^{230}Th/^{232}Th$ ratio with depth indicates that some seawater-derived Th was added to the particles during their settling.

## 4. Discussion

### 4.1. The role of water circulation in the transport of $^{230}Th$

At the Gibraltar Strait, Atlantic surface water enters the Alboran Sea and flows in the western Mediterranean Sea as Modified Atlantic Water (MAW) where it follows a cyclonic path that produces the Liguro–Provençal current along the Riviera [18]. MAW occupies the upper 150 m of the water column. Some surface water flows through the Sicily strait in the Eastern basin. Levantine Intermediate Water (LIW) enters the western basin through the Sicily Strait [19]. At the DYFAMED site, LIW is found around 500 m. It follows a cyclonic path and leaves eventually the Western basin for the Alboran Sea and the Gibraltar Strait. The North Western Mediterra-

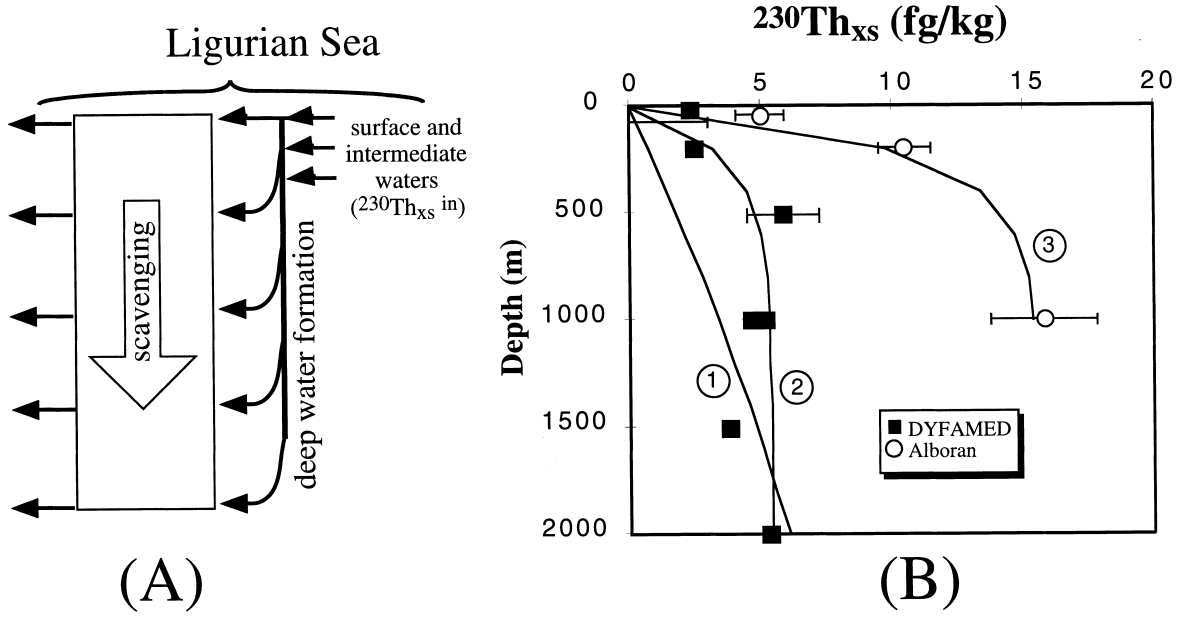


Fig. 3. Principle and result of the advection–scavenging model. (A) Schematic representation of the model: Th is carried by the reversible scavenging on particles and by lateral advection of water. A mixture of surface and intermediate waters is introduced uniformly throughout the water column and this flow is balanced by the lateral removal of seawater at the same rate. (B) Measured and modeled total $^{230}Th_{xs}$ profiles. DYFAMED: filled squares: $^{230}Th_{xs}$ measured in unfiltered samples. Curve 1: $\tau_w = 4.5$ yr and $\tau_s = 20$ yr. Curve 2: $\tau_w = 20$ yr and $\tau_s = 4.5$ yr. Alboran Sea: open circles: $^{230}Th_{xs}$ measured in unfiltered samples. Curve 3: $\tau_w = 20$ yr and $\tau_s = 50$ yr.

nean Deep Waters (NWMDW) are formed during winter in the Gulf of Lyon and in the Ligurian Sea where dense waters can reach the seafloor [20,21]. They are found below the LIW and down to the seafloor. They also follow a cyclonic path. Some deep waters are uplifted in the Alboran Sea and they flow in the Atlantic Ocean through the Gibraltar Strait [22].

The transport of $^{230}$Th is often modeled by considering a system at steady state where the in situ production is balanced by a reversible scavenging on settling particles and where water mass transport can be neglected [6,9,23]. In this case, a linear increase of dissolved and particulate $^{230}$Th with depth is expected and often observed. The $^{230}Th_{xs}$ profiles in the Alboran Sea and at DYFAMED are not linear and they have different Th levels. Since the production rate of $^{230}$Th by in situ radioactive decay of $^{234}$U is almost constant in seawater, it reflects differences in scavenging and transport of Th. The ventilation of the water column produces $^{230}$Th profiles with constant concentrations at depth when the renewal time of the water ($\tau_W$) is short compared to the $^{230}$Th residence time with respect to scavenging for the entire water column ($\tau_s$) [24]. We apply a conceptual model derived from [24] to the ventilation of the western basin. We assume that (Fig. 3A):

- Th is carried throughout the water column by reversible scavenging on particles at a rate $\tau_s^{-1}$.
- the water column is renewed at all depths by surface and intermediate waters introduced uniformly at a rate $\tau_w^{-1}$ and that this flow is balanced by the lateral removal of seawater at the same rate. We consider that the $^{230}Th_{xs}$ concentration of the inflowing water is $^{230}Th_{xs}^{in} = 2.5$ fg/kg (corresponding to the 20–200 m values at DYFAMED).

The transport equation is:

$$\frac{d^{230}Th_{xs}}{dt} = -\frac{h}{2\tau_s}\frac{d^{230}Th_{xs}}{dz} - \frac{1}{\tau_w}(^{230}Th_{xs}^{in} - ^{230}Th_{xs}) + P \quad (2)$$

where $h$ is the water column depth and $P$ ($= 0.65$ fg/kg) is the in situ production rate. Assuming a steady state ($d^{230}Th_{xs}/dt = 0$), the evolution of the $^{230}Th_{xs}$ concentrations with depth ($z$) is given by:

$$^{230}Th_{xs} = (^{230}Th_{xs}^{in} + P\tau_w) \times \left(1 - \exp\left(-\frac{2\tau_s}{\tau_w}\frac{z}{h}\right)\right) \quad (3)$$

At DYFAMED, a reasonable fit of the data is obtained with $\tau_w = 4.5$ yr and $\tau_s = 20$ yr (Fig. 3B). It is not possible to adjust properly the model to the data with $\tau_w = 20$ yr and $\tau_s = 4.5$ yr, because it yields a quasi-linear profile (scavenging is much faster than ventilation). The deep water renewal time of 4.5 yr is short compared to water residence time in the Algero–Provençal basin. The $\tau_w$ value estimated at DYFAMED may not be representative of the whole basin because DYFAMED is close to or even within the zone of deep water formation (deep waters are formed through small chimneys that are difficult to observe and deep waters formed elsewhere in the Ligurian Sea may feed the DYFAMED area through lateral transport). Similarly, a short renewal time (11 yr) of the Deep Western basin based on tritium data in the Gulf of Lyon was explained by the efficient ventilation in this area [25].

On the contrary, the Alboran Sea receives intermediate and deep waters just before they flow out of the Algero–Provençal basin. The high $^{230}Th_{xs}$ concentrations found in the Alboran Sea (Fig. 3B) reflect larger values of $\tau_w$ ($\tau_w = 20$ yr) and $\tau_s$ ($\tau_s = 50$ yr). This value of $\tau_w$ agrees with the estimated residence time of deep water in the Algero–Provençal basin but is much larger than the water residence time in the Alboran sea itself based on salt and heat budget ($\tau_w \sim 0.5$ yr [19]). Therefore, the $^{230}$Th concentrations in the Alboran Sea reflect the scavenging history experienced by NWMDW and LIW before their arrival in the Alboran Sea and the mixing between MAW, LIW and NWMDW.

The $^{230}Th_{xs}$ content of the deep water is controlled by the ventilation rate rather than by scavenging ($\tau_w^{-1} \gg \tau_s^{-1}$). Therefore a change in $\tau_w$ over

several years should have an impact on the $^{230}Th_{xs}$ content of the deep water. It suggests that $^{230}Th_{xs}$ can be used as a tracer of the deep water formation rate.

### 4.2. The cycling of dissolved and colloidal Thorium

In marine environments, truly dissolved Th is rapidly adsorbed on colloidal particles [26]. The long residence time of Th in seawater reflects the residence time of these colloids with respect to aggregation on larger particles [27]. $^{234}Th$ has been extensively used to study the fate of colloidal matter [17]. $^{230}Th$ and $^{232}Th$ are used here to gain further insight in the colloid thorium dynamics. The $^{230}Th/^{232}Th$ ratios of the $<1$ kDa fraction are close to the $^{230}Th/^{232}Th$ ratios of filtered samples (although the agreement is not very good at 1000 m, possibly due to a slight contamination). It is remarkable that the in situ-produced $^{230}Th$ is not strongly enriched in the $<1$ kDa fraction compared to the lithogenic $^{232}Th$. Therefore the colloidal material does not seem strongly enriched in lithogenic material and an equilibrium must exist between truly dissolved and colloidal Th to ensure this similarity of $^{230}Th/^{232}Th$ ratio. An upper limit to the time required to establish this equilibrium is given by sum of the colloid residence time (5–50 days) and of the sample storage (1 month). Scavenging rates of truly dissolved Th derived from irreversible scavenging models may be underestimated because this equilibrium is not taken into account [17].

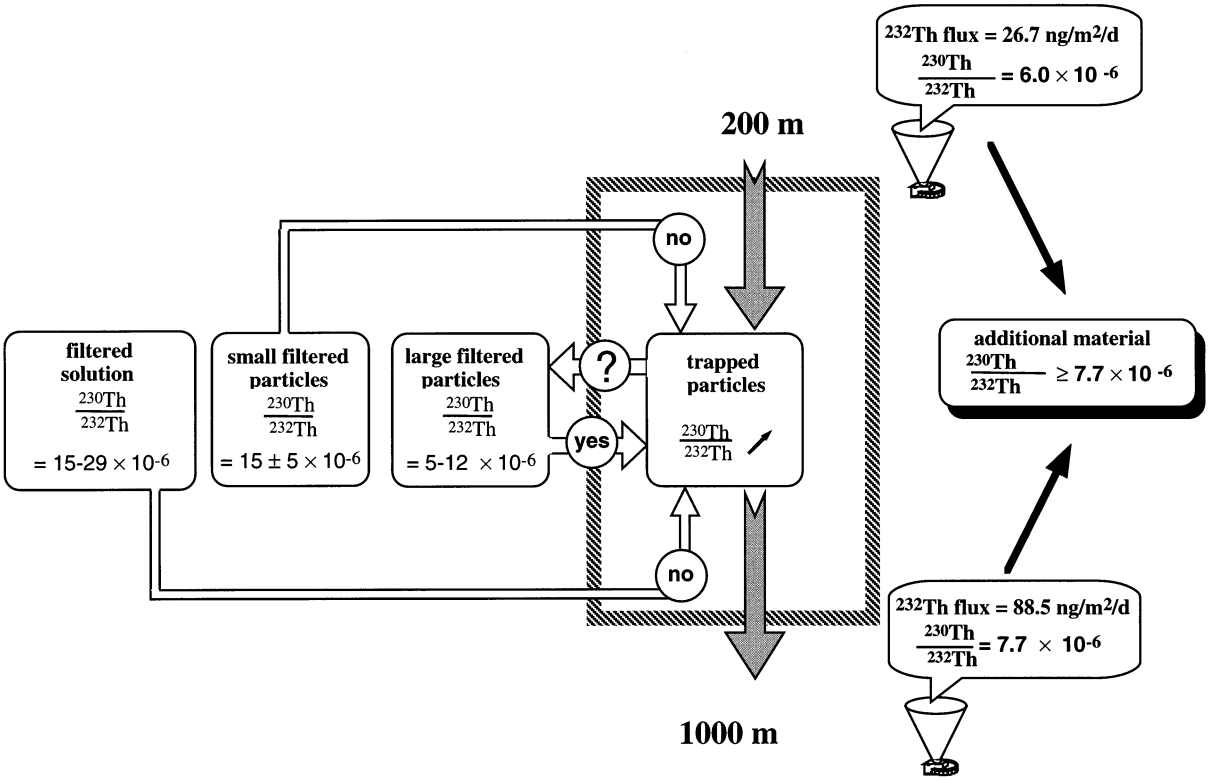


Fig. 4. Schematic evolution of the vertical Th flux between 200 m and 1000 m. The increase of $^{232}Th$ flux and the shift of $^{230}Th/^{232}Th$ ratio in the sediment trap between 200 m and 1000 m require an addition of thorium with an average isotopic ratio of $^{230}Th/^{232}Th = (8.2 \pm 0.8) \times 10^{-6}$. Among the possible sources, the reservoir of the filtered large particles is the only one that fulfils Th and Pb isotope conditions.

### 4.3. Evolution of the particulate matter flux at DYFAMED

When the particulate matter falls through the water column, it experiences changes through processes such as aggregation or disaggregation. Understanding these changes is important for the present carbon budget as well as for many paleoproxy calibrations. Here, we use the $^{230}Th/^{232}Th$ ratio to evaluate the influence of aggregation on the evolution of the particle flux. We focus on the August/September period for which we have seawater, filtered and trapped particle data (Fig. 4). The increase of the mass flux with depth does not reflect only aggregation–disaggregation because the mass flux is also modified by organic matter mineralization. Because there is little particulate Th dissolution [15], the increase of Th flux represents the net effect between aggregation, disaggregation and adsorption of dissolved Th. We call $\phi$ the fraction of $^{232}Th$ in the material trapped at 1000 m that was aggregated between 200 and 1000 m. If no disaggregation occurred, $\phi = (F^{232}_{1000m} - F^{232}_{200m})/F^{232}_{1000m} = 70\%$ and if the particles sinking from 200 m were fully disaggregated before reaching 1000 m, $\phi = 100\%$. The $^{230}Th/^{232}Th$ ratio of trapped particles changed from $6.0\times10^{-6}$ at 200 m to $7.7\times10^{-6}$ at 1000 m indicating that Th with $^{230}Th/^{232}Th = 7.7\times10^{-6}$ was added to trapped particles. We consider that Th in the 1000 m trapped particles is a mixture of Th from the 200 m trapped particles and from an additional reservoir (seawater, small particles or filtered large particles, Fig. 4). If $\theta$ and $(1-\theta)$ are the $^{232}Th$ fractions from the additional reservoir and from the 200 m trapped particles in the mixture, $\theta$ is determined independently of the flux data by:

$$\theta = \frac{\left(\frac{^{230}Th}{^{232}Th}\right)_M - \left(\frac{^{230}Th}{^{232}Th}\right)_B}{\left(\frac{^{230}Th}{^{232}Th}\right)_A - \left(\frac{^{230}Th}{^{232}Th}\right)_B} \quad (4)$$

The fractions of additional Th are $\theta_{seawater} = 7$–$19\%$, $\theta_{SFP} = 12$–$100\%$ and $\theta_{LFP} = 28$–$100\%$ if the additional Th was provided by seawater, small or filtered large particles respectively. By comparing $\theta$ and $\phi$, it appears that the direct adsorption of dissolved Th cannot satisfy both isotopic and flux balances. On the other hand, both small and filtered large particles can satisfy these balances. Pb isotope data obtained on the same sediment trap samples argue against an extensive aggregation of small filtered particles on the settling particles at this site and during this particular time series [28]. Therefore, only filtered large particles can represent the additional source of material to the trapped particles. It appears that filtered large particles, that are rarely sampled or considered in particle transport models, play a key role in the evolution of the trapped flux. The apparent settling velocity of filtered large particles due to aggregation on trapped particles is $^{232}Th_{LPF}/F^{232}_{aggr} = 8$–$80$ m/day where $^{232}Th_{LFP}$ is the average concentration in seawater of $^{232}Th$ associated to filtered large particles and $F^{232}_{aggr}$ is the flux of $^{232}Th$ aggregated onto trapped particles between 200 m and 1000 m. This is significantly larger than the settling speed of small particles $v = h/(2\times\tau_s\times0.2) = 0.7$ m/day that can be derived from the ventilation/scavenging model considering that 20% of $^{230}Th$ is carried by small particles.

To evaluate $\phi$, we assumed that both traps had the same collection efficiency. Low trapping efficiencies are often observed for shallow traps [29,30] and the increase of the $^{232}Th$ flux between 200 and 1000 m could reflect a low trapping efficiency of the 200 m trap. However, during the August period, the currents measured at 200 and 1000 m are $< 2$ cm/s (J.-C. Miquel, personal communication) whereas low trapping efficiencies are observed mostly for higher current speed [31,32].

Finally, it must be noted that $^{232}Th$ fluxes increasing with depth in the Atlantic Ocean are attributed to the lateral transport of particulate matter from the continental margin rather than to trapping efficiency problems [33]. Similarly, material transported from the slope could contribute to the material aggregated on trapped particles at DYFAMED. It would have strong implications for the particulate flux study at DYFAMED (in particular for particulate organic carbon), because only vertical particulate transport is considered usually at this station.

Table 5
Thorium fluxes to the western Mediterranean Sea

| | Water flux ($10^6$ kg/s) | $^{232}$Th (pg/kg) | $^{230}$Th (fg/kg) | Particle flux ($10^6$ g/s) | $^{232}$Th (μg/g) | $^{230}$Th (pg/g) | $^{232}$Th flux (g/s) | $^{230}$Th flux ($10^{-6}$ g/s) |
|---|---|---|---|---|---|---|---|---|
| Gibraltar Strait | 1110 | 45 | 2 | | | | 0.049 | 2. 2 |
| Sicily Strait | 1242 | 439 | 6.3 | | | | 0.52 | 7.5 |
| Rivers (dissolved) | 3.3 | 100 | 0.5 | | | | 0.0003 | 0.0015 |
| Rivers (particulate) | | | | 1.5 | 10 | 44 | 15 | 67 |
| Aerosols | | | | 0.38 | 10 | 44 | 3.8 | 17 |
| In situ production | | | | | | | | 29 |
| Dissolved from particles[a] | | | | | | | $0.9 \pm 0.3$ | $4.0 \pm 1.5$ |

[a] See text for calculation. Water and particulate matter fluxes are taken from [19,35]. $^{230}$Th and $^{232}$Th data are from [12,14,36] and from this work for the LIW flowing from the eastern basin. $^{230}$Th concentrations of riverine and eolian material based on a ratio $^{230}Th/^{232}Th = 4.4 \times 10^{-6}$ [14]. In situ production of $^{230}$Th ($= 3.25$ dpm/l $= 0.65$ fg/l/yr) is estimated from $^{234}$U concentration in Mediterranean waters [37] and the volume of the western Mediterranean Sea ($1.42 \times 10^6$ km$^3$).

### 4.4. Dissolution of lithogenic particulate inputs in the western Mediterranean Sea

The natural sources and the dissolution extent of lithogenic matter and the resulting fluxes of refractory elements to the Mediterranean Sea or to the ocean are poorly constrained [34]. Here, we present an original method to evaluate the flux of $^{232}$Th in seawater by dissolution of lithogenic material. The average $^{230}Th/^{232}Th$ ratio of the western basin is the result of the external fluxes of $^{230}$Th and $^{232}$Th and of the in situ production of $^{230}$Th (Table 5). Eolian and riverine particulate matter provides the largest Th fluxes but only a small fraction of this particulate Th is dissolved in seawater. The riverine flux of particulate Th given in Table 5 corresponds to the total load of the rivers, but only 10% of this load reaches the open sea, the remaining 90% being trapped on margins [35]. It is not known if this sequestered material contributes to the budget of dissolved Th. The main flux of dissolved $^{230}$Th is due to in situ production so that it is precisely known and the flux of dissolved $^{232}$Th can be precisely determined by calibration with the $^{230}$Th flux. At steady state, the mean $^{230}Th/^{232}Th$ ratio of the western basin is:

$$\left(\frac{^{230}\mathrm{Th}}{^{232}\mathrm{Th}}\right)_{\mathrm{W.B.}} = \frac{P_T + F_G\,{}^{230}\mathrm{Th}_G + F_S\,{}^{230}\mathrm{Th}_S + F_{rd}\,{}^{230}\mathrm{Th}_{rd} + (F_{eol} + AF_{rp})^{230}\mathrm{Th}_{litho} D}{F_G\,{}^{232}\mathrm{Th}_G + F_S\,{}^{232}\mathrm{Th}_S + F_{rd}\,{}^{232}\mathrm{Th}_{rd} + (F_{eol} + AF_{rp})^{232}\mathrm{Th}_{litho} D} \quad (5)$$

where $F_G$, $F_S$ and $F_{rd}$ are the water fluxes from the Gibraltar Strait, the Sicily Strait and the rivers; $F_{eol}$ and $F_{rp}$ are the flux of eolian and riverine particles; $Th_G$, $Th_S$ and $Th_{rd}$ are the concentrations in the Atlantic, Levantine Intermediate and river waters; $Th_{litho}$ is the Th concentration in the lithogenic material; $A$ is the fraction of riverine particles that interact with seawater; $D$ is the fraction of Th dissolution from the particles (we assume that it is the same for riverine and eolian inputs) and $P_T$ is the total $^{230}$Th in situ production in the basin.

The average $^{230}Th/^{232}Th$ ratio is $24 \times 10^{-6}$ at DYFAMED and $35 \times 10^{-6}$ in the Alboran Sea deep water. We consider that $24 \times 10^{-6} < (^{230}Th/^{232}Th)_{\text{western med}} < 35 \times 10^{-6}$. From Eq. 5, we obtain the flux of $^{232}$Th dissolved from particles: $(F_{eol} + AF_{rp}) \times {}^{232}Th_{litho} \times D = 0.92 \pm 0.33$ g/s. It represents 23% of the eolian flux and 6% of the riverine particle flux, but it is the main dissolved $^{232}$Th flux. This flux is determined independently of the eolian and riverine particulate Th fluxes and of the extent of particle dissolution: the accuracy of this value is limited by our knowledge of the $(^{230}Th/^{232}Th)_{\text{western med}}$ ratio and of the Sicily strait $^{232}$Th flux (which is of similar magnitude). If $A = 10\%$ (all atmospheric and only 10%

of riverine inputs interact with seawater), we deduce that $D = 11–23\%$ (a large dissolution extent is required) whereas if $A = 100\%$ (all atmospheric and riverine inputs interact with seawater), $D = 3–5\%$ (a smaller dissolution extent is required). Experimental dissolution of lithogenic-rich marine particle suggests that $D = 2\%$ [15]. The percentage of Th from the eolian dusts that is dissolved when it enters seawater is not known, but it is less than 10% for Al [38] and less than 2% for rare earth elements [39]. Thorium being more refractory than Al and rare earth elements, it seems that dissolution of particulate Th is limited. Therefore, we consider that dissolution of a small fraction of all the riverine particulate load (including particles sequestered in margins) is required to explain the $^{230}Th$–$^{232}Th$ budget of the western Mediterranean sea. While the transport of particulate lithogenic material is viewed as mainly one-dimensional at DYFAMED, the budgets of dissolved refractory elements require to take lateral advection into account. This conclusion probably holds for other refractory elements and the Mediterranean budgets of elements such as Fe, Nd and Mn require revision [34,40,41]. This Th budget emphasizes that at the ocean scale, the inputs of refractory elements may not be controlled only by eolian fluxes as previously proposed [42] but that lateral transport from margins must be taken into account.

## 5. Conclusion

We report the first extensive $^{230}Th$ and $^{232}Th$ data set measured on size-fractionated seawater and marine particle samples from the western Mediterranean Sea. The $^{230}Th/^{232}Th$ ratio provides information that are not accessible to concentrations or single isotope measurements when mixing processes (reversible scavenging on colloids, aggregation–disaggregation, etc.) are involved. The Th particulate flux evolution requires to take into account the aggregation of filtered large particles that are rarely sampled or considered in the models of particle dynamics. The $^{230}Th$–$^{232}Th$ budget of the western Mediterranean Sea suggests that the external fluxes of refractory elements (Th, Fe, Nd and Mn) are dominated by the dissolution of the continental particles stored in margins and not only by eolian input as usually assumed. It stresses that at the ocean scale, the inputs of refractory elements are not controlled by eolian fluxes only but that inputs from shelves must be considered. This is of particular importance in the ongoing debate concerning the respective role of eolian and advective inputs of Fe in the limitation of the present and past ocean productivity [43–45].

## Acknowledgements

We are grateful to J.C. Marty for his support to our project at the DYFAMED station. We thank the captain and the crew of the R.V. *Professeur Georges Petit* for their assistance and hospitality during the cruise. We thank B. Dupré and J. Viers for sharing their expertise on ultrafiltration systems, R. Arraes-Mescoff and K. Tachikawa for providing already-dissolved aliquots particulate samples, J.-C. Miquel for the current-meter data, C. Jeandel, C. Bournot-Marec, M. Benkiram, O. Radakovitch and R. Sempéré for their help during the sampling and P. Brunet for maintaining the mass spectrometer in good shape. We are grateful to C. Jeandel for her constant support and her constructive criticisms. The manuscript benefited of the constructive comments from B. Hamelin, G. Henderson and an anonymous reviewer. This work was supported by the DYFAMED (PROOF/INSU) operation and by the European Program MATER.*[AH]*

## References

[1] J.C. Miquel, P. Buat-Ménard, S.W. Fowler, J. LaRosa, Dynamics of the downward flux of particles and carbon in the open northwestern Mediterranean Sea, Deep-Sea Res. 41 (1994) 243–261.

[2] S.W. Fowler, P. Buat-Ménard, Y. Yokohama, S. Ballestra, E. Holm, H.V. VanNguyen, Rapid removal of Chernobyl fallout from Mediterranean surface waters by biological activity, Nature 329 (1987) 56–58.

[3] P. Buat-Ménard, J. Davies, E. Remoudaki, J.C. Miquel, G. Bergametti, C.E. Lambert, U. Ezat, C. Quetel, J. LaRosa, S.W. Fowler, Non steady state removal of atmo-

spheric particles from Mediterranean surface waters, Nature 340 (1989) 131–134.
[4] D.P. Ruiz-Pino, C.E. Lambert, C. Jeandel, P. Buat-Ménard, Modelling the biogenic transport of atmospheric particles in the Mediterranean Sea, Global Planet. Change 3 (1990) 47–65.
[5] S. Schmidt, P. Nival, J.-L. Reyss, M. Baker, P. Buat-Menard, Relation between 234Th scavenging and zooplancton biomass in Mediterranean surface waters, Oceanol. Acta 15 (1992) 227–231.
[6] M. Roy-Barman, J.H. Chen, G.J. Wasserburg, $^{230}$Th-$^{232}$Th systematics in the Central Pacific Ocean: the sources and the fates of thorium, Earth Planet. Sci. Lett. 139 (1996) 351–363.
[7] A.J. Spivack, J.H. Chen, G.J. Wasserburg, Neodymium and thorium in the Mediterranean, EOS 67 (1986) 1066.
[8] C.J. Beets, G.J. Wasserburg, J.H. Chen, G.J. De Lange, Depleted 238U and excess 234U and 230Th: enhanced disequilibrium of U-series isotopes in hypersaline mediterranean brines, in: M.A. Lanphere, G.R. Dalrumple, B.D. Turrin (Eds.), ICOG 8, U.S. Geological Survey Circular 1107 25, 1994.
[9] M.P. Bacon, R.F. Anderson, Distribution of thorium isotopes between dissolved and particulate forms in the deep-sea, J. Geophys. Res. 87 (1982) 2045–2056.
[10] H. Grout, R. Sempéré, A. Thill, A. Calafat, L. Prieur, M. Canals, Morphological and chemical variability of colloids in the Almeria-Oran Front in the eastern Alboran Sea (SW Mediterranean Sea): evidence by means of analytical electron microscopy, Limnol. Oceanogr. 46 (2001) 1347–1357.
[11] J.L. Banner, G.J. Wasserburg, J.H. Chen, C.H. Moore, 234U-238U-230Th-232Th systematics in saline groundwaters from central Missouri, Earth Planet. Sci. Lett. 101 (1990) 296–312.
[12] S. Volger, J. Scholten, M. Rutgers van der Loeff, A. Mangini, $^{230}$Th in eastern North Atlantic: the importance of water ventilation in the balance of $^{230}$Th, Earth Planet. Sci. Lett. 156 (1998) 47–61.
[13] A. Mangini, R.M. Key, A $^{230}$Th profile in the Atlantic Ocean, Earth Planet. Sci. Lett. 62 (1983) 377–384.
[14] P.S. Andersson, G.J. Wasserburg, J.H. Chen, D.A. Papanastassiou, J. Ingri, $^{238}$U-$^{234}$U and $^{232}$Th-$^{230}$Th in the Baltic sea and in river water, Earth Planet. Sci. Lett. 130 (1995) 217–234.
[15] R. Arraes-Mescoff, L. Coppola, M. Roy-Barman, M. Souhaut, K. Tachikawa, C. Jeandel, R. Sempéré, C. Yoro, The behavior of Al, Mn, Ba, Sr, REE and Th isotopes during in vitro bacterial degradation of large marine particles, Mar. Chem. 73 (2001) 1–19.
[16] M. Dai, K.O. Buesseler, P. Ripple, J. Andrews, R.A. Belastock, O. Gustafsson, S.B. Moran, Evaluation of 2 cross-flow ultrafiltration membranes for isolating marine organic colloids, Mar. Chem. 62 (1998) 117–136.
[17] L. Guo, P.H. Santchi, Composition and cycling of colloids in marine environments, Rev. Geophys. 35 (1997) 17–40.
[18] C. Millot, Circulation in the Western Mediterranean Sea, J. Mar. Syst. 20 (1999) 432–442.
[19] J.P. Béthoux, B. Gentili, The Mediterranean Sea, coastal and deep-sea signatures of environmental changes, J. Mar. Syst. 20 (1999) 383–394.
[20] J.-P. Béthoux, Mean water fluxes across sections in the Mediterranean Sea, evaluated on the basis of water and salt budgets and of observed salinities, Oceanol. Acta 3 (1980) 79–88.
[21] G.P. Gasparini, G. Zodiatis, M. Astraldi, C. Galli, S. Sparnocchia, Winter Intermediate water lenses in the Ligurian Sea, J. Mar. Syst. 20 (1999) 319–332.
[22] T.H. Kinder, G. Parrilla, Yes. Some of the Mediterranean outflow does come from great depth, J. Geophys. Res. 92 (C3) (1987) 2901–2906.
[23] Y. Nozaki, Y. Horibe, H. Tsubota, The water column distribution of thorium isotopes in the western North Pacific, Earth Planet. Sci. Lett. 54 (1981) 203–216.
[24] M.M. Rutgers van der Loeff, G.W. Berger, Scavenging of 230Th and 231Pa near the Antarctic Polar Front in the South Atlantic, Deep-Sea Res. 40 (1993) 339–357.
[25] C. Andrié, L. Merlivat, Tritium in the western Mediterranean Sea during the Phycemed cruise, Deep-Sea Res. 35 (1988) 247–267.
[26] S.E.H. Niven, P.E. Kepkay, J.B.C. Bugden, The role of TEP in 234Th dynamics during a coastal diatom bloom, Radioprotection 32 (1996) 213–218.
[27] B.D. Honeyman, P.H. Santschi, A brownian-pumping model for oceanic trace metal scavenging: evidence from Th isotopes, J. Mar. Res. 47 (1989) 951–992.
[28] L.Y. Alleman, B. Hamelin, A.J. Véron, J.C. Miquel, S. Heussner, Lead sources and transfer in the coastal Mediterranean evidence for stable lead isotopes in marine particles, Deep-Sea Res. 47 (2000) 2257–2279.
[29] K.O. Buesseler, Do upper-ocean sediment traps provide an accurate record of particle flux?, Nature 353 (1991) 420–423.
[30] K.O. Buesseler, M.P. Bacon, J.K. Cochran, H.D. Livingston, Carbon and nitrogen export during the JGOFS North Atlantic Bloom Experiment estimated from 234Th238U disequilibria, Deep-Sea Res. 39 (1992) 1115–1137.
[31] W.D. Gardner, Sediment trap dynamics and calibration: a laboratory evaluation, J. Mar. Res. 38 (1980) 17–39.
[32] E.T. Baker, H.B. Milburn, D.A. Tennant, Field assessment of sediment trap efficiency under varying flow conditions, J. Mar. Res. 46 (1988) 573–592.
[33] P.G. Brewer, Y. Nozaki, D.W. Spencer, A.P. Fleer, Sediment trap experiment in the deep North Atlantic: isotopic and elemental fluxes, J. Mar. Res. 38 (1980) 703–728.
[34] C. Guieu, R. Chester, M. Nimmo, J.-M. Martin, S. Guerzoni, E. Nicolas, J. Mateu, S. Keyse, Atmospheric input of dissolved and particulate metals the northwestern Mediterranean, Deep-Sea Res. 44 (1997) 655–674.
[35] J.M. Martin, F. Elbaz-Poulichet, C. Guieu, M.D. Loye-Pilot, G. Han, River versus atmospheric input of material

to the Mediterranean Sea: an overview, Mar. Chem. 28 (1989) 159–182.
[36] S.R. Taylor, S.M. McLennan, The Continental Crust: Its Composition and Evolution, Blackwell, Oxford, 1985, 312 pp.
[37] S. Schmidt, J.-L. Reyss, Concentrations en uranium des eaux méditerranéennes de salinitées élevées, C. R. Acad. Sci. 312 (1991) 479–484.
[38] H.B. Maring, R.A. Duce, The impact of atmospheric aerosols on trace metal geochemistry in open ocean surface seawater, 1. Aluminium, Earth Planet. Sci. Lett. 84 (1987) 381–392.
[39] M.J. Greaves, P.J. Statham, H. Elderfield, Rare earth element mobilization from marine atmospheric dust into seawater, Mar. Chem. 46 (1994) 255–260.
[40] F. Henry, C. Jeandel, J.-F. Minster, Particulate and dissolved Nd in the Western Mediterranean Sea: sources, fates and budget, Mar. Chem. 45 (1994) 283–305.
[41] G. Sarthou, C. Jeandel, Seasonal variations of iron concentrations in the Ligurian Sea and iron budget in the western Mediterranean Sea, Mar. Chem. 74 (2000) 115–129.
[42] C.-A. Huh, W.S. Moore, D.C. Kadko, Oceanic 232Th: A reconnaissance and implications of global distribution from manganese nodules, Geochim. Cosmochim. Acta 53 (1989) 1357–1366.
[43] K.S. Johnson, M.R. Gordon, K.H. Coale, What controls dissolved iron in the world ocean?, Mar. Chem. 57 (1997) 137–161.
[44] E. Boyle, What controls dissolved iron in the world ocean? A comment, Mar. Chem. 57 (1997) 163–167.
[45] G.W.I. Luther, J. Wu, What controls dissolved iron in the world ocean? A comment, Mar. Chem. 57 (1997) 173–179.